

Controlling the asymptotic bias of the unadjusted (Microcanonical) Hamiltonian and Langevin Monte Carlo

Jakob Robnik^{*} , and Uroš Seljak^{*,†}

Abstract. Hamiltonian and Langevin Monte Carlo (HMC and LMC) and their Microcanonical counterparts (MCHMC and MCLMC) are current state of the art algorithms for sampling in high dimensions. Their numerical discretization errors are typically corrected by the Metropolis-Hastings (MH) accept/reject step. However, as the dimensionality of the problem increases, the stepsize (and therefore efficiency) needs to decrease as $d^{-1/4}$ for second order integrators in order to maintain reasonable acceptance rate. The MH unadjusted methods, on the other hand, do not suffer from this scaling, but the difficulty of controlling the asymptotic bias has hindered the widespread adoption of these algorithms. For Gaussian targets, we show that the asymptotic bias is upper bounded by the energy error variance per dimension (EEVPD), independently of the dimensionality and of the parameters of the Gaussian. We numerically extend the analysis to the non-Gaussian benchmark problems and demonstrate that most of these problems abide by the same bias bound as the Gaussian targets. Controlling EEVPD, which is easy to do, ensures control over the asymptotic bias. We propose an efficient algorithm for tuning the stepsize, given the desired asymptotic bias, which enables usage of unadjusted methods in a tuning-free way.

MSC2020 subject classifications: Primary 65P99.

Keywords: Hamiltonian Monte Carlo, Error analysis.

1 Introduction

Sampling represents a bottleneck for various scientific problems, ranging from quantum chromodynamics and statistical physics to economics and Bayesian inference. The necessity for samplers arises when computing expectation values of functions $\langle f \rangle_p = \int p(\mathbf{x})f(\mathbf{x})d\mathbf{x}$, where $f(\mathbf{x})$ is some function of the high dimensional parameters \mathbf{x} and $p(\mathbf{x}) = e^{-\mathcal{L}(\mathbf{x})}/Z$ is a given probability density, with a possibly unknown normalization constant Z . A general class of sampling models is Monte Carlo Markov Chain (MCMC). Here, a Markov chain $\{\mathbf{x}_i\}_{i=1}^n$ is designed such that after discarding a sufficient number k of burn-in samples, distribution average $\langle f \rangle_p$ can be approximated by the time average over the chain $\langle f \rangle_{MCMC} = \frac{1}{n-k} \sum_{i=k+1}^n f(\mathbf{x}_i)$. A gold standard algorithm in situations with available gradient $\nabla \mathcal{L}(\mathbf{x})$ is Hamiltonian Monte Carlo [6, 17, 1], where the Markov transition is determined by randomly drawing the velocity from a standard Gaussian, $u_i \sim \mathcal{N}(0, 1)$, and then simulating the Hamiltonian dynamics with the Hamiltonian

^{*}Physics Department, University of California, Berkeley, USA , jakob_robnik@berkeley.edu

[†]Lawrence Berkeley National Laboratory, Berkeley, USA , useljak@berkeley.edu

$H(\mathbf{x}, \mathbf{u}) = \frac{1}{2}|\mathbf{u}|^2 + \mathcal{L}(\mathbf{x})$. A related dynamics with similarly good sampling properties is that of underdamped Langevin Monte Carlo [13], where the full velocity refreshment is replaced by a partial refreshment $u_i \sim \mathcal{N}(\sqrt{1 - \eta^2}u_i, \eta)$.

Generically, Hamiltonian dynamics cannot be simulated exactly, so a numerical integrator like leapfrog [13] is used to approximate it. The integrator’s error is typically corrected by treating Hamiltonian dynamics simulation as a proposal in the Metropolis-Hastings (MH) accept/reject step, with the acceptance probability $\min(1, e^{-E})$, where E is the energy difference between the previous state and the generated proposal. Note that the energy is a constant of motion for the exact Hamiltonian dynamics, so the proposals are always accepted if the integration accuracy is sufficiently good. However, generating good integration accuracy is computationally expensive, so a tradeoff needs to be established, for example the optimal acceptance rate was shown to be 65% for product targets [18]. Metropolis adjusted HMC is attractive because it has no asymptotic bias, meaning that the estimates $\langle f \rangle_{MCMC}$ are asymptotically unbiased. Furthermore, users do not need to hand-tune the stepsize, which can instead be determined by targeting the desired acceptance rate in a short prerun. However, acceptance rate can only be on order one if the energy variance is also on the order one [18]. Therefore, as the dimensionality of the problem increases, the stepsize (and therefore efficiency) needs to decrease as $d^{-1/4}$. In high dimensional problems, this is a prohibitive cost, that can potentially be avoided by not doing the MH adjustment, while ensuring that the bias is smaller than the variance. In practice, the effective sample size, which determines the variance, is typically of order $n_{eff} \sim 100 - 1000$, implying that the squared bias must be below $0.02 - 0.002$ for the bias to be negligible.

In some fields with high dimensional configuration spaces, like Molecular Dynamics (MD), the unadjusted methods are used almost exclusively, and the standard choice is underdamped Langevin Monte Carlo (LMC). Domain knowledge and trial runs are used to select an appropriate stepsize, which ensures a sufficiently small asymptotic bias [13]. Another option is to run multiple chains with decreasing stepsize to show that expectation values do not depend on the stepsize below some limit [4]. However, a more efficient way of selecting the stepsize would be to select one which ensures a certain predetermined level of asymptotic bias.

Another recently introduced class of algorithms is Microcanonical Hamiltonian Monte Carlo (MCHMC) [21], which is a sampling algorithm that utilizes the fixed energy Hamiltonian dynamics, as opposed to Hamiltonian Monte Carlo (HMC) [6, 17], which operates at different energy levels under the canonical distribution. MCHMC Hamiltonian function is chosen to ensure that the marginal of the microcanonical distribution on the constant-energy-surface over the momentum variables matches the desired target distribution. MCHMC typically outperforms HMC in direct comparison tests [21]. In analogy to Langevin dynamics one can also consider partial velocity refreshments, denoted MCLMC [22]. [21] numerically demonstrated that the asymptotic bias is related to the error in energy variance per dimension (EEVPD). It was found that the relation between the asymptotic bias and EEVPD appears to depend only weakly on the problem dimensionality, even for the non-Gaussian targets.

In this work, we explore analytically the relation between EEVPD and the asymptotic bias for the Gaussian targets with leapfrog integrator. In section 3 we show that both asymptotic Wasserstein distance error and covariance matrix error can be upper bounded by EEVPD, independently of the parameters of the Gaussian and its dimensionality. This relation can in turn be used to adaptively determine the stepsize. Such an adaptation algorithm based on the energy error was proposed in [21]: estimate EEVPD by running the dynamics for a certain number of steps, adjust the stepsize according to the scaling of the energy error with the stepsize and repeat until convergence. This method can be accelerated by adaptively changing the stepsize based on the current best guess for the optimal stepsize, instead of waiting at a fixed stepsize to obtain a satisfactory estimate of EEVPD. In general, some form of stochastic optimization with vanishing adaptation [20, 18] is used in this setting, such as the dual averaging algorithm in NUTS [9]. The convergence in these algorithms is achieved by the time decaying weights. Since the stepsize tuning is usually performed during the unsteady state of the burn-in, we argue that time-decaying weights are suboptimal, as was also noted in [9]. Instead, we want the most recent samples to contribute the most to the average. We present such an algorithm in Section 4. In Section 5 we derive the energy error and the bias of the unadjusted MCHMC dynamics and compare it to HMC. In Section 6 we numerically confirm the analytical results and examine the applicability of the Gaussian upper bound to the non-Gaussian targets.

2 Setup

We study the Gaussian target distribution, $p(\mathbf{x}) \propto e^{-\mathcal{L}(\mathbf{x})}$, with

$$\mathcal{L}(\mathbf{x}) = \frac{1}{2} \mathbf{x}^T H \mathbf{x}. \tag{1}$$

Here, Hessian H is a positive definite $d \times d$ matrix and $\mathbf{x} \in \mathbb{R}^d$ is a vector of configuration space parameters. Hessian inverse is $\Sigma = H^{-1} = \langle \mathbf{x} \otimes \mathbf{x} \rangle_p$, which is the covariance matrix. In general, we will denote by $\langle f \rangle_q$ the expectation of f over distribution q . We will assume that we have a black box access to $\mathcal{L}(\mathbf{x})$ and $\nabla \mathcal{L}(\mathbf{x})$, but no other prior knowledge.

Unadjusted algorithms approximate the Hamiltonian dynamics with an update map

$$(\mathbf{x}_{t+\epsilon}, \mathbf{u}_{t+\epsilon}) \approx \Phi_\epsilon(\mathbf{x}_t, \mathbf{u}_t), \tag{2}$$

where ϵ is the stepsize of the algorithm. The Markov transition kernel is then a composition of these update maps and a momentum refreshment

$$T = \mathcal{R} \circ \Phi_\epsilon \circ \Phi_\epsilon \circ \dots \circ \Phi_\epsilon. \tag{3}$$

In HMC and MCHMC, the momentum refreshment is $\mathcal{R}(\mathbf{u}) = \mathbf{z}$ and $\mathcal{R}(\mathbf{u}) = \mathbf{z}/|\mathbf{z}|$, respectively, where $\mathbf{z} \sim \mathcal{N}(0, I)$. In LMC and MCLMC, $\mathcal{R}(\mathbf{u}) = \sqrt{1 - \eta^2} \mathbf{u} + \eta \mathbf{z}$ and $\mathcal{R}(\mathbf{u}) = (\mathbf{u} + \eta \mathbf{z})/|\mathbf{u} + \eta \mathbf{z}|$, respectively, and only a single copy of Φ_ϵ is typically used in

Eq. (3). The approximate update Φ_ϵ produces some energy error, which for HMC and LMC equals

$$\Delta E = \frac{1}{2}(\mathbf{x}_{t+\epsilon}^T H \mathbf{x}_{t+\epsilon} + |\mathbf{u}_{t+\epsilon}|^2 - \mathbf{x}_t^T H \mathbf{x}_t - |\mathbf{u}_t|^2). \quad (4)$$

After the burn-in, the samples are distributed according to the stationary distribution $p_\infty(\mathbf{x})$, which differs from $p(\mathbf{x})$ for unadjusted samplers. The stationary distribution depends on ϵ , the stepsize of the integration algorithm used. No matter how many samples we collect, the accuracy of our expectation values will be limited by this asymptotic bias. We will define an error $b(p, p_\infty)$ as a measure of the discrepancy between p and p_∞ . We will have some requirements for b :

1. $b \geq 0$ and $b(p, p) = 0$. Small b should imply higher accuracy of the expectation values that we would like to compute.
2. Making multiple copies of the same distribution does not change the error: $b(p \otimes p, p_\infty \otimes p_\infty) = b(p, p_\infty)$.
3. Simultaneously rescaling $\mathbf{x} \rightarrow a\mathbf{x}$ and $\epsilon \rightarrow a\epsilon$ does not change the error. Rotating the coordinate system does not change the error.

We will use two metrics that satisfy these conditions, Wasserstein and Covariance error.

2.1 Wasserstein error

Commonly used in the mathematical literature, Wasserstein distance $W_2(p, q)$ between two probability densities p and q is the cost of transporting one density to the other,

$$W_2(p, q)^2 = \inf_{\pi \in \Pi(p, q)} \int |\mathbf{x} - \mathbf{x}'|^2 \Pi(\mathbf{x}, \mathbf{x}') d\mathbf{x} d\mathbf{x}', \quad (5)$$

where $\Pi(p, q)$ is the set of probability densities on $\mathbb{R}^d \times \mathbb{R}^d$ with marginals p and q . Wasserstein distance provides an upper bound on the error of certain expectation values, in particular the mean of the posterior distribution [7, 12].

If we make multiple copies of the distribution, Wasserstein distance grows as a square root of the number of copies, so we will be interested in W_2^2/d , to satisfy requirement 2. We define

$$b_W^2 = \frac{W_2^2}{d} \frac{1}{\epsilon^2}, \quad (6)$$

which satisfies requirement 3 as well. We will now list some special cases which will be of use later. If both p and q are Gaussian with the same mean and covariance matrices Σ_p and Σ_q , the Wasserstein distance simplifies to [19]

$$W_2^2 = \text{Tr} \left\{ \Sigma_p + \Sigma_q - 2(\Sigma_p^{1/2} \Sigma_q \Sigma_p^{1/2})^{1/2} \right\}. \quad (7)$$

Furthermore, if Σ_q is of the form: $\Sigma_q = \Sigma_p + \epsilon^n R$, where n is a positive integer and R is some ϵ -independent matrix which commutes with Σ_p , then

$$W_2^2 = \text{Tr} \left\{ 2\Sigma_p + \epsilon^n R - 2\Sigma_p(1 + \epsilon^n \Sigma_p^{-1} R)^{1/2} \right\} \quad (8)$$

$$= \frac{\epsilon^{2n}}{4} \text{Tr}\{\Sigma_p^{-1} R^2\} + \mathcal{O}(\epsilon^{2n+2}).$$

2.2 Covariance error

A more direct measure of the sampling accuracy [8] is the squared error of the variance estimate:

$$b_{\text{diag}}^2 = \frac{1}{d} \sum_{i=1}^d \left(1 - \frac{\text{Var}[x_i]_{p_\infty}}{\text{Var}[x_i]_p}\right)^2. \quad (9)$$

More generally, we define the covariance matrix error as

$$b_\Sigma^2 \equiv \frac{1}{d} \text{Tr}\{(1 - \Sigma_p^{-1} \Sigma_{p_\infty})^2\}. \quad (10)$$

b_{diag} and b_Σ coincide for the diagonal matrices and are rescaling invariant, but b_Σ also penalizes the error of the off-diagonal elements and is rotationally invariant. In Appendix A we show that requirement 1 is satisfied. Both b are related to the effective sample size, $b^2 = 2/n_{\text{eff}}$, see Appendix A, which implies requirement 2.

3 Hamiltonian and Langevin Monte Carlo

The stationary distribution of unadjusted HMC and LMC with stepsize ϵ was shown in [16] to be

$$p_\infty(\mathbf{x}, \mathbf{u}) \propto \exp\left\{-\frac{1}{2} \mathbf{x}^T H_\infty \mathbf{x}\right\} \exp\left\{-\frac{1}{2} \mathbf{u}^T \mathbf{u}\right\}, \quad (11)$$

where

$$H_\infty \equiv H \left(1 - \frac{\epsilon^2}{4} H\right). \quad (12)$$

The covariance error Eq. (10) of the stationary distribution (11) is:

$$b_\Sigma^2 = \frac{1}{d} \text{Tr}\left\{\left(1 - (1 - \epsilon^2 H/4)^{-1}\right)^2\right\} = \frac{1}{d} \text{Tr}\left\{\left(\sum_{n=1}^{\infty} (\epsilon^2 H/4)^n\right)^2\right\} = \frac{\epsilon^4}{16} \frac{\text{Tr}\{H^2\}}{d} + \mathcal{O}(\epsilon^8), \quad (13)$$

whereas the Wasserstein error Eq. (6) is

$$b_W^2 = \frac{W_2^2}{d} \frac{1}{\epsilon^2} = \epsilon^2 \text{Tr}\{H/d\}/4. \quad (14)$$

We would like to compare these errors with the energy error Eq. (4). The update map Φ_ϵ in leapfrog (Verlet) integration is given by

$$\begin{aligned} \mathbf{x}_{t+\epsilon} &= \left(1 - \frac{1}{2} \epsilon^2 H\right) \mathbf{x}_t + \epsilon \left(1 - \frac{1}{4} \epsilon^2 H\right) \mathbf{u}_t \\ \mathbf{u}_{t+\epsilon} &= -\epsilon H \mathbf{x}_t + \left(1 - \frac{1}{2} \epsilon^2 H\right) \mathbf{u}_t \end{aligned} \quad (15)$$

for the position leapfrog integrator and

$$\begin{aligned}\mathbf{x}_{t+\epsilon} &= \left(1 - \frac{1}{2}\epsilon^2 H\right)\mathbf{x}_t + \epsilon\mathbf{u}_t \\ \mathbf{u}_{t+\epsilon} &= \epsilon\left(-H + \frac{1}{4}\epsilon^2 H^2\right)\mathbf{x}_t + \left(1 - \frac{1}{2}\epsilon^2 H\right)\mathbf{u}_t\end{aligned}\tag{16}$$

for the velocity leapfrog integrator. Inserting in Equation (4) results in massive cancellations, yielding

$$\Delta E = \pm \frac{1}{4}\epsilon^3 \mathbf{u}^T H^2 \mathbf{x} + \mathcal{O}(\epsilon^4),\tag{17}$$

where plus (minus) sign corresponds to the velocity (position) Verlet. We will be interested in the energy error variance per dimension (EEVPD):

$$\text{Var}[E]/d = (\langle \Delta E^2 \rangle - \langle \Delta E \rangle^2)/d,\tag{18}$$

which is a quantity that can easily be determined in the experiment. At the leading order, it will not matter if the expectation values are taken in the stationary distribution or in the target distribution. We get the same results for both Verlet integrators:

$$\begin{aligned}\langle \Delta E \rangle^2 &= \mathcal{O}(\epsilon^8) \\ \text{Var}[E]/d &= \frac{\epsilon^6}{16d} \langle (\mathbf{u}^T H^2 \mathbf{x})^2 \rangle = \frac{\epsilon^6}{16d} \langle u_a u_b \rangle \langle x_c x_d \rangle H_{ac}^2 H_{bd}^2 = \frac{\epsilon^6}{16} \text{Tr}\{H^3\}/d,\end{aligned}\tag{19}$$

where Einstein's summation convention is used for repeated indices. Comparing this expression with the asymptotic errors b_W and b_Σ yields our main result

$$\text{Var}[E]/d = 4b^3 \Delta(H),\tag{20}$$

where for b_W

$$\Delta(H) = \frac{\text{Tr}\{H^3/d\}}{(\text{Tr}\{H/d\})^3},\tag{21}$$

and for b_Σ

$$\Delta(H) = \frac{\text{Tr}\{H^3/d\}}{(\text{Tr}\{H^2/d\})^{3/2}}.\tag{22}$$

If $\Delta = 1$ (as it would be for example for the standard Gaussian target $H = I$), this relation guarantees an asymptotic error of 10% if we have $\text{Var}[E]/d = 0.004$. In general, we can bound $\Delta \geq 1$, by the Jensen inequality. Therefore, taking $\Delta = 1$ is the most pessimistic situation and we get $b < 0.1$ if $\text{Var}[E]/d = 0.004$.

4 Stepsize adaptation

We now develop a practical algorithm for tuning the step size ϵ in a sequential algorithm. Suppose we did a leapfrog step with size ϵ_k and found some energy error ΔE_k . Using

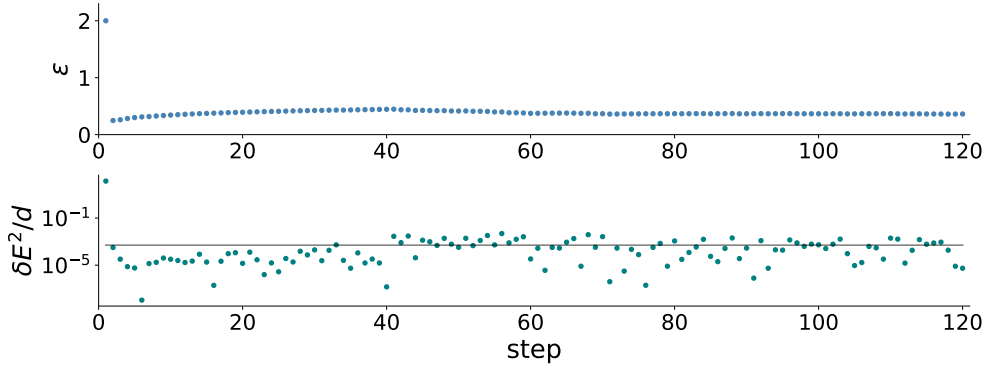


Figure 1: The stepsize adaptation algorithm from Section 4, applied to the Rosenbrock target distribution in $d = 36$, with $Q = 0.1$ from [21]. The sequential algorithm was initialized from the standard Gaussian distribution with a random initial velocity orientation. Top: the stepsize as a function of leapfrog integration steps. Bottom: per dimension squared energy error for each step. The algorithm quickly converges to the targeted EEVPD = 0.001, shown with a black line.

only this knowledge and the scaling from Equation (19), we could estimate the optimal step size as $\epsilon = \xi_k^{-1/6}$ where

$$\xi_k = \frac{\Delta E_k^2}{d} \frac{1}{\alpha \epsilon_k^6} \quad (23)$$

and α is the desired EEVPD, typically taken on the order of 10^{-3} , but this choice will depend on the desired accuracy. As we do more leapfrog steps, we can improve our estimate by averaging energy errors and use the predicted optimal stepsize in the next step:

$$\epsilon_{n+1} = \left(\frac{\sum_{k=1}^n w(\xi_k) \gamma^{n-k} \xi_k}{\sum_{k=1}^n w(\xi_k) \gamma^{n-k}} \right)^{-1/6}. \quad (24)$$

We have introduced two types of weights:

- The weights w parametrize our trust in the predictions from the too large and too small ϵ . We take the log-normal penalty

$$w(\xi) = \exp\left\{-\frac{1}{2}(\log \xi)^2 / \sigma_\xi^2\right\}, \quad (25)$$

with $\sigma_\xi = 1.5$.

- γ is the forgetting factor. It is related to the effective sample size n of the estimate (if w were constant) by $\gamma = \frac{n-1}{n+1}$. n is also the number of steps after which the weights have decayed to $e^{-2} = 0.13$. In general, we don't want n to be too small, so that EEVPD is well determined and yet not too large during the burn-in such

that the initially heavily biased estimates are forgotten quickly. We find $n = 50$ to work well on all benchmark tests from [21]. An example run is shown in Figure 1.

The pseudocode for the proposed algorithm is shown in 1.

Data: initial condition (\mathbf{x}, \mathbf{u}) ,
initial step size $\epsilon > 0$,
number of integration steps $N > 0$,
desired EEVPD $\alpha > 0$.
Result: stepsize ϵ
 $A, B \leftarrow 0$;
for $n \leftarrow 0$ **to** N **do**
 $(\mathbf{x}, \mathbf{u}), \Delta E \leftarrow \Phi_\epsilon(\mathbf{x}, \mathbf{u})$;
 $\xi \leftarrow \text{Equation (23)}(\Delta E, \epsilon, \alpha)$;
 $A \leftarrow A\gamma + \xi w(\xi)$;
 $B \leftarrow B\gamma + w(\xi)$;
 $\epsilon \leftarrow (A/B)^{-1/6}$;
end

Algorithm 1: Stepsize adaptation

5 Microcanonical Hamiltonian and Langevin Monte Carlo

MCHMC dynamics in the natural parametrization targets the isokinetic distribution $p(\mathbf{x}, \mathbf{u}) \propto e^{-\mathcal{L}(\mathbf{x})} \delta(|\mathbf{u}|^2 - 1)$. The dynamics is governed by the differential equations for \mathbf{x} and the unit velocity \mathbf{u} :

$$\begin{aligned} \frac{d}{dt} \mathbf{x}_t &= \mathbf{u}_t \\ \frac{d}{dt} \mathbf{u}_t &= -\frac{1}{d-1} (I - \mathbf{u}_t \mathbf{u}_t^T) \nabla \mathcal{L}(\mathbf{x}_t). \end{aligned} \quad (26)$$

Position leapfrog integrator [15, 24, 21] approximates this dynamics by

$$\begin{aligned} \mathbf{x}_{t+\epsilon/2} &= \mathbf{x}_t + \frac{\epsilon}{2} \mathbf{u}_t \\ \mathbf{u}_{t+\epsilon} &= \frac{\mathbf{u}_t + (\sinh \delta + \mathbf{e} \cdot \mathbf{u}_t (\cosh \delta - 1)) \mathbf{e}}{\cosh \delta + \mathbf{e} \cdot \mathbf{u}_t \sinh \delta} \\ \mathbf{x}_{t+\epsilon} &= \mathbf{x}_t + \frac{\epsilon}{2} (\mathbf{u}_t + \mathbf{u}_{t+\epsilon}) \\ E_\epsilon(\mathbf{z}) &= (d-1) \log \left[\cosh \delta + \mathbf{e} \cdot \mathbf{u}_t \sinh \delta \right] + \frac{1}{2} \mathbf{x}_{t+\epsilon}^T H \mathbf{x}_{t+\epsilon} - \mathbf{x}_t^T H \mathbf{x}_t, \end{aligned} \quad (27)$$

where $\mathbf{e} = -H\mathbf{x}_{t+\epsilon/2}/|H\mathbf{x}_{t+\epsilon/2}|$ and $\delta = \epsilon|H\mathbf{x}_{t+\epsilon/2}|/(d-1)$. Expanding the energy error after one leapfrog step to the third order in ϵ gives

$$E_\epsilon = \epsilon^3 \left(\frac{(\mathbf{u}^T H \mathbf{u})(\mathbf{x}^T H \mathbf{u}) - (\mathbf{x}^T H^2 \mathbf{u})}{4(d-1)} + \frac{(\mathbf{x}^T H \mathbf{u})^3 - (\mathbf{x}^T H^2 \mathbf{x})(\mathbf{x}^T H \mathbf{u})}{6(d-1)^2} \right). \quad (28)$$

We will compute EEVPD for MCHMC, but unfortunately, a result analogous to (11) is not known, so we will not be able to directly compare EEVPD with the asymptotic errors. To nevertheless estimate the asymptotic errors, we will assume the ensemble of particles is distributed according to the target distribution and then only a single leapfrog step is performed on each particle. The resulting distribution will serve as an approximation to p_∞ . This will obviously underestimate the asymptotic bias, but it can still be used as a comparison between HMC and MCHMC if the same approximation is also used in HMC.

The stepsize ϵ is not directly comparable between MCHMC and HMC, because in MCHMC, the velocity norm is exactly one, while the HMC, velocity lies on a typical set of a standard Gaussian, so its magnitude has small fluctuations around \sqrt{d} . We define a rescaled stepsize \mathcal{E} which can be used to directly compare the step sizes of the algorithms. For MCHMC and MCLMC, $\mathcal{E} = \epsilon/\sqrt{d}$, whereas $\mathcal{E} = \epsilon$ for HMC and LMC.

EEVPD is given by Equation (28) squared, averaged over the target distribution. Averaging is performed by the Wick's theorem [10, 25, 11, 14], the details are in Appendix B. The result is

$$\begin{aligned} \text{Var}[E]/d &= \epsilon^6 \left((-17+d) \text{Tr}\{H\}^3 - 6(-3-2d+d^2) \text{Tr}\{H\} \text{Tr}\{H^2\} \right. \\ &\quad \left. + (32+38d+33d^2+9d^3) \text{Tr}\{H^3\} \right) / 144(-1+d)^3 d^2 (2+d)(4+d) \\ &\stackrel{d \gg 1}{\approx} \frac{\mathcal{E}^6}{144} \left(\text{Tr}\{H/d\}^3 - 6 \text{Tr}\{H/d\} \text{Tr}\{H^2/d\} + 9 \text{Tr}\{H^3/d\} \right), \end{aligned} \quad (29)$$

where $\stackrel{d \gg 1}{\approx}$ denotes asymptotic equality in the limit $d \rightarrow \infty$. Similarly, we expand the covariance matrix after one step to the fourth order in ϵ and use the results from Appendix B to get

$$\Sigma_{ij} = \langle [\mathbf{x}_\epsilon]_i [\mathbf{x}_\epsilon]_j \rangle = H_{ij}^{-1} - \frac{\epsilon^4}{12d(d-1)(d+2)} \left((3d+4)H_{ij} - \text{Tr}\{H\}\delta_{ij} \right). \quad (30)$$

The corresponding covariance matrix error is

$$b_\Sigma^2 = \frac{\mathcal{E}^8}{144} \left(9 \text{Tr} H^4/d - 6 \text{Tr} H/d \text{Tr} H^3/d + (\text{Tr} H/d)^4 \right). \quad (31)$$

By assuming that the ensemble distribution is still Gaussian after one step, but with the wrong covariance matrix we can also estimate the Wasserstein error

$$b_W^2 = \frac{\mathcal{E}^6}{576} \left(9 \text{Tr} H^3/d - 6 \text{Tr} H/d \text{Tr} H^2/d + (\text{Tr} H/d)^3 \right). \quad (32)$$

Comparing these errors with EEVPD gives

$$\text{Var}[E]/d = \frac{1}{4} b_W^2 = \frac{b_\Sigma^{3/2}}{\sqrt{6}} \Delta(H), \quad (33)$$

where

$$\Delta(H) = \frac{\frac{9}{4} \text{Tr}\{H^3/d\} - \frac{6}{4} \text{Tr}\{H/d\} \text{Tr}\{H^2/d\} + \frac{1}{4} \text{Tr}\{H/d\}^3}{\left(\frac{9}{4} \text{Tr}\{H^4/d\} - \frac{6}{4} \text{Tr}\{H/d\} \text{Tr}\{H^3/d\} + \frac{1}{4} \text{Tr}\{H/d\}^4\right)^{3/4}}.$$

We have a worst worst-case, H -independent bound, which we prove in the Appendix C:

Lemma 5.1. $0.37d^{-1/4} \leq \Delta(H) \leq 3.1$.

5.1 Analogous results for HMC and LMC

Here we derive the corresponding results for HMC and LMC. The two-point correlation function after one step of (15) is

$$\begin{aligned} \langle x'_i x'_j \rangle_{p_0}^{(\text{position})} &= [(H^{-1} - \epsilon^2/2)(1 - \epsilon^2 H/2)]_{ij} + \epsilon^2 [(1 - \epsilon^2 H/4)^2]_{ij} = H_{ij}^{-1} - \epsilon^4 H_{ij}/4 + \mathcal{O}(\epsilon^6) \\ \langle x'_i x'_j \rangle_{p_0}^{(\text{velocity})} &= [(H^{-1} - \epsilon^2/2)(1 - \epsilon^2 H/2)]_{ij} + \epsilon^2 \delta_{ij} = H_{ij}^{-1} + \epsilon^4 H_{ij}/4, \end{aligned} \quad (34)$$

because the cross terms vanish in expectation, yielding the errors

$$b_W^2 = \frac{\epsilon^6}{64} \text{Tr}\{H^3/d\} \quad b_\Sigma^2 = \frac{\epsilon^8}{16} \text{Tr}\{H^4/d\}, \quad (35)$$

Which are related to the energy error (19) by

$$\text{Var}[E]/d = 4b_W^2 = \frac{b_\Sigma^{3/2}}{2} \Delta(H), \quad (36)$$

where

$$\Delta(H) = \frac{\text{Tr}\{H^3/d\}}{(\text{Tr}\{H^4/d\})^{3/4}}. \quad (37)$$

In general we can bound $d^{-1/4} \leq \Delta \leq 1$.

5.2 Comparison

EEVPD and error scaling are the same way for all algorithms:

$$\text{Var}[E]/d \propto \mathcal{E}^6 \quad b_W^2 \propto \mathcal{E}^6 \quad b_\Sigma^2 \propto \mathcal{E}^8, \quad (38)$$

where the proportionality constants depend on the (unknown) Hessian, but not directly on the dimensionality d . For MCHMC this confirms the optimal scaling $\epsilon \propto \sqrt{d}$ as proposed in [21]. The energy error-asymptotic bias relations are similar for all algorithms, despite the Hessian dependence of the prefactors in (38) being considerably different:

$$\text{Var}[E]/d = C_W b_W^2 = C_\Sigma(H) b_\Sigma^{3/2}. \quad (39)$$

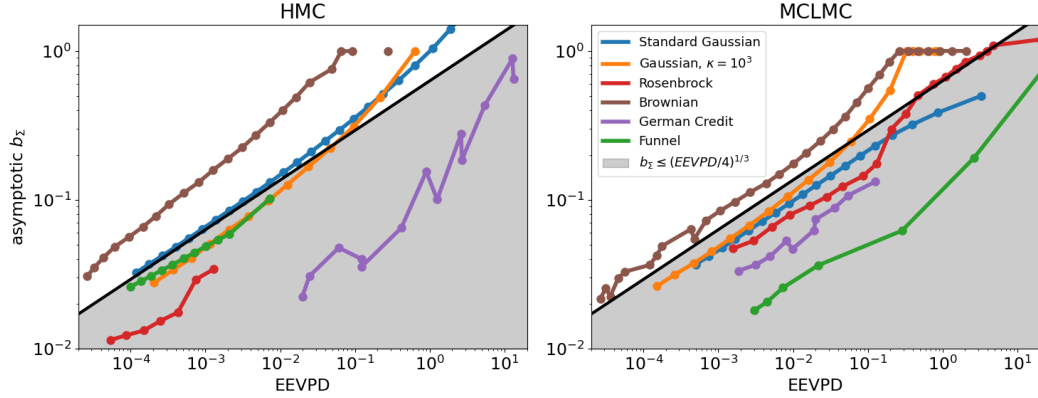


Figure 2: Asymptotic covariance matrix error b_Σ as a function of the energy error EEVPD. Unadjusted HMC is shown on the left and unadjusted MCLMC on the right. The relation is shown for various inference problems from Section 6. The analytical equality for the Standard Gaussians at small stepsizes from Equation (20) is shown in black. The inequality for Gaussian distributions at small stepsizes is shown as a shaded grey region. Most non-Gaussian targets also abide by this inequality.

C_W and $C_\Sigma(H)$ are typically on the order one, and the worst case bound for $C_\Sigma(H)$ is of the form $d^{-1/4} \lesssim C_\Sigma \lesssim 1$. Interestingly, the energy variance in one leapfrog step is directly related to the Wasserstein distance travelled in this step in the distribution space, independently of the Hessian of the problem and the dynamics used (HMC or MCHMC). The similar form of these results for HMC and MCHMC suggests that EEVPD in MCHMC might also be related to its proper asymptotic bias, so the adaptation algorithm from Sec. 4 could also be used in MCHMC.

We can compare the algorithms in terms of the distance travelled / gradient evaluation at a fixed one-step bias. For a standard Gaussian ($H = I$), using Eq. (31) and (35), we get at a fixed covariance matrix error:

$$\frac{\text{distance traveled by MCHMC} / \text{gradient eval}}{\text{distance traveled by HMC} / \text{gradient eval}} = \frac{\epsilon_{MCHMC}}{\epsilon_{HMC}\sqrt{d}} = \left(\frac{9}{4}\right)^{1/8} \approx 1.11, \quad (40)$$

and at fixed Wasserstein error, $(9/4)^{1/6} \approx 1.14$. This suggests that MCHMC is a slightly more efficient sampler, but in practice a larger difference has been observed [21].

6 Numerical experiments

So far we have focused on Gaussian targets and even then, our main bias-EEVPD relation from Equation (20) relies on the Taylor expansion, rendering it valid only in the limit of small stepsize. Here we will study its validity for a realistic range of stepsizes, for standard non-Gaussian benchmark problems.

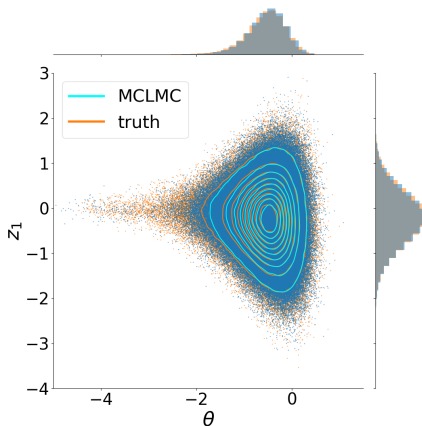


Figure 3: Posterior density for the funnel problem. 2d marginal distribution in the $\theta - z_1$ plane and the corresponding 1d marginals are shown. The contours are obtained by the kernel density estimation, the samples are shown as dots. The ground truth, obtained by a very long NUTS chain is shown in orange, unadjusted MCLMC is shown in blue. Both chains are 10^7 samples long to eliminate the variance error. The two methods give practically indistinguishable posteriors, demonstrating that the discretization bias was successfully suppressed by the EEVPD control.

We study five benchmark problems:

- Standard Gaussian in $d = 100$. This is a sanity check that the equality (20) applies exactly when the stepsize is small.
- Ill-conditioned Gaussian in $d = 100$ and condition number $\kappa = 1000$. The eigenvalues of the covariance matrix are equally spaced in log. This is as a sanity check that the inequality (20) applies exactly, when the stepsize is small.
- Direct sum of 16 Rosenbrock functions with $Q = 0.1$ from [8]. This is a banana shaped target in 32 dimensions, see Figure 8 in [21].
- Brownian motion example from the Inference Gym [23], where it is named `BrownianMotionUnknownScalesMissingMiddleObservations`. This is a 32 dimensional hierarchical Bayesian model where Brownian motion with unknown innovation noise and measurement noise is fitted to the noisy and partially missing data.
- German credit example from the Inference gym, where it is named `GermanCreditNumericSparseLogisticRegression`. This is a 51 dimensional hierarchical Bayesian model with one hierarchical parameter, where sparse logistic regression is used to model the approval of the credit based on the information about the applicant.

- Funnel problem is a 101 dimensional hierarchical Bayesian model with a funnel shape [8]. The goal is to infer the hierarchical parameter θ and the latent variables $\{z_i\}_{i=1}^{100}$, given the noisy observations $y_i \sim \mathcal{N}(z_i, 1)$. The prior is the Neal’s funnel [18]: $\theta \sim \mathcal{N}(0, 3)$, $z_i \sim \mathcal{N}(0, e^{\theta/2})$. We set $\theta_{\text{true}} = 0$ and generate the data with the generative process described above. Given this data we then sample from the posterior for θ and $\{z_i\}_{i=1}^{100}$.

The ground truth covariance matrix for the first two problems is known exactly. For the Rosenbrock function, we compute it by drawing exact samples from the posterior. For the last three problems, we obtain the ground truth by running extremely long NUTS chains. For the funnel problem we set the acceptance rate to the unusually high level of 95%, because NUTS otherwise fails to explore the narrow throat part of the funnel.

For each problem, we run unadjusted chains with different stepsizes, each chain using 10^8 gradient calls. We eliminate the initial 10^4 calls as a burn-in and use the consecutive samples to compute the expectation values for the covariance matrix and EEVPD. We monitor b_Σ from Equation (10) and check that it has converged to the asymptotic value. If the convergence has not yet been achieved, we eliminate these measurements from the plots. This happens for some of the harder problems at small stepsizes, where the chains are not long enough. We show the asymptotic value of b_Σ as a function of EEVPD in Figure 2, with results averaged over 4 independent chains. Numerical results for unadjusted HMC on Gaussian distributions agree perfectly with the analytical results of Equation (20). The inequality also applies to the majority of non-Gaussian benchmark problems. One exception is the Brownian motion example, where it is off by approximately a factor of 1.5 at small stepsizes, meaning that one would think one has $< 2\%$ asymptotic error, when in fact it was 3%. Rosenbrock function example is only shown at small stepsizes, because the problem becomes numerically unstable at higher stepsizes, incurring divergences. Even though the asymptotic error-EEVPD relation (20) was derived for HMC it seems to apply approximately for MCLMC as well, so an EEVPD-based adaptation of the stepsize could be used for both algorithms.

In Figure 3 we show the posterior density for the funnel problem, obtained by the unadjusted MCLMC algorithm. We required $b = 0.01$ asymptotic bias and used Equation (20) to get the corresponding EEVPD = 4×10^{-6} . We then used Algorithm 1 to determine the MCLMC stepsize. The resulting posterior is practically indistinguishable from a very long NUTS chain, demonstrating that the discretization error is indeed very small.

7 Conclusion

In this paper we make progress in connecting the asymptotic bias of MH unadjusted gradient based samplers (HMC, LMC, MCHMC, MCLMC) to the energy error arising from the discretization of Hamiltonian dynamics. While our analytical results are only applicable to the Gaussian targets, they provide theoretical justification for the notion that in high dimensions MH unadjusted methods are computationally advantageous

over MH adjusted methods. In many of the computationally most challenging sampling applications such as lattice QCD the dimensionality of the problem can exceed 10^8 [3, 2, 5], which would lead to a factor of 100 or more reduction of computational time over the standard Metropolis adjusted HMC. The practical implications of our work extend to various domains where unadjusted methods are employed for sampling tasks, enabling more informed choices of algorithmic parameters and minimizing the bias in sampling results.

Acknowledgments

We thank Qijia Jiang for proving Lemma 5.1.

Funding

This material is based upon work supported in part by the Heising-Simons Foundation grant 2021-3282 and by the U.S. Department of Energy, Office of Science, Office of Advanced Scientific Computing Research under Contract No. DE-AC02-05CH11231 at Lawrence Berkeley National Laboratory to enable research for Data-intensive Machine Learning and Analysis.

Appendix A: Covariance matrix error

We have defined the error of the covariance matrix estimate Σ as

$$b_{\Sigma}^2 = \frac{1}{d} \text{Tr}\{R^2\}, \quad (41)$$

where $R = I - H\Sigma$, see Equation (10). We will first prove that this definition is reasonable:

Lemma A.1. b_{Σ}^2 is non-negative.

Proof. Trace of a squared matrix is not positive in general (counterexample is a rotation by $\pi/2$ in two dimensions), we will have to use the fact that H and Σ are positive-definite matrices. Without loss of generality, we may assume that Σ is diagonal with positive entries, because the trace is invariant under the change of basis and Σ must be diagonal in some basis because it is positive-definite. R then has $R_{ii} = 1 - H_{ii}\Sigma_{ii}$ on the diagonal and $R_{ij} = -H_{ij}\Sigma_{jj}$ off the diagonal. The trace is

$$\text{Tr}\{R^2\} = \sum_{i=1}^d (1 - H_{ii}\Sigma_{ii})^2 + \sum_{i \neq j} H_{ij}\Sigma_{jj}H_{ji}\Sigma_{ii},$$

where the first and the second term are the contribution from the diagonal and off-diagonal elements respectively. The first term is non-negative because it is a sum of squares. The second term is non-negative because all factors Σ_{ii} , Σ_{jj} and $H_{ij}H_{ji} = (H_{ij})^2$ are non-negative. \square

Note that we could also take the more transparently non-negative definition $b_F^2 = \frac{1}{d} \text{Tr}\{RR^T\} = \frac{1}{d} \|R\|_F^2$, where $\|\cdot\|_F$ is the Frobenius norm. However, b_F^2 cannot be related

to the effective sample size in a Hessian independent way. We will now show that b_Σ^2 can be. Suppose we had n_{eff} i.i.d exact samples from the target distribution $\mathbf{x}^{(k)} \sim \mathcal{N}(0, H^{-1})$. We will denote the expectation with respect to the sample realizations by $\mathbb{E}[\cdot]$. Our estimate of the covariance matrix

$$\Sigma_{ab} = \frac{1}{n} \sum_{k=1}^n x_a^{(k)} x_b^{(k)} \quad (42)$$

is unbiased

$$\mathbb{E}[\Sigma_{ab}] = H_{ab}^{-1} \quad (43)$$

and has the covariance

$$\mathbb{E}[\Sigma_{ab}\Sigma_{cd}] = H_{ab}^{-1}H_{cd}^{-1} + \frac{1}{n_{\text{eff}}} (H_{ac}^{-1}H_{bd}^{-1} + H_{ad}^{-1}H_{bc}^{-1}). \quad (44)$$

The estimate's expected bias under both definitions is then $2/n_{\text{eff}}$:

$$\begin{aligned} \mathbb{E}[b_{\text{diag}}^2] &= 1 - 2\frac{1}{d} \sum_{i=1}^d \frac{\langle \Sigma_{ii} \rangle}{H_{ii}^{-1}} + \frac{1}{d} \sum_{i=1}^d \frac{\langle \Sigma_{ii}^2 \rangle}{(H_{ii}^{-1})^2} = \frac{2}{n_{\text{eff}}} \\ \mathbb{E}[b_\Sigma^2] &= 1 - 2\frac{1}{d} H_{ij} \langle \Sigma_{ij} \rangle + \frac{1}{d} H_{ij} \langle \Sigma_{jk} \Sigma_{li} \rangle H_{kl} = \frac{2}{n_{\text{eff}}}. \end{aligned} \quad (45)$$

Appendix B: Averaging formalism

To obtain EEVPD and an estimate of the asymptotic bias in Section 5, we will need to compute averages over the target distribution: Gaussian distribution over the configuration space variables \mathbf{x} and uniform distribution on the sphere over the velocity variables \mathbf{u} . Gaussian expectation values are computed by the Wick's theorem, which relates the higher moments of the Gaussian distribution to its two point correlation function $\langle x_i x_j \rangle = H_{ij}^{-1}$. Wick's theorem states that the n -point correlation functions are given by all possible pairwise contractions. So for example,

$$\langle x_i x_j x_k x_l \rangle = H_{ij}^{-1} H_{kl}^{-1} + H_{ik}^{-1} H_{jl}^{-1} + H_{il}^{-1} H_{jk}^{-1}. \quad (46)$$

There are three terms corresponding to three contractions $(i-j, k-l)$, $(i-k, j-l)$ and $(i-l, j-k)$. For the n -point correlation function, with even n , let's denote the number of contractions by $N_n = (n-1)!!$.

Expectation with respect to the uniform distribution on the hypersphere

$$p(\mathbf{u}) = \frac{1}{V(S^{d-1})} \delta(|\mathbf{u}| - 1) \quad (47)$$

is closely related to the moments of the standard Gaussian distribution,

$$\langle x_{i_1} x_{i_2} \cdots x_{i_n} \rangle_{\mathcal{N}(0,1)} = \int dr \frac{e^{-r^2/2}}{(2\pi)^{d/2}} \int_{S^{d-1}} (ru_{i_1})(ru_{i_2}) \cdots (ru_{i_n}) d\Omega_{d-1} = \langle r^n \rangle \langle u_{i_1} u_{i_2} \cdots u_{i_n} \rangle, \quad (48)$$

We will need the following diagrams, which we now compute:

$$\begin{aligned}
\langle (\mathbf{x}^T H^2 \mathbf{u})^2 \rangle &= \left| \frac{3}{2} \right| \left| \frac{3}{2} \right| = \frac{\text{Tr}\{H^3\}}{d} \\
\langle (\mathbf{x}^T H \mathbf{u})(\mathbf{x}^T H^2 \mathbf{u})(\mathbf{u}^T H \mathbf{u}) \rangle &= \left| \frac{3}{2} \right| \left| \frac{1}{2} \right| \sqcup_1 = \sqcup_2 \sqcup_1 \\
\langle (\mathbf{x}^T H^2 \mathbf{x})(\mathbf{x}^T H^2 \mathbf{u})(\mathbf{x}^T H \mathbf{u}) \rangle &= \overset{1}{\sqcap} \left| \frac{3}{2} \right| \left| \frac{1}{2} \right| = \overset{1}{\sqcap} \overset{2}{\sqcap} \\
\langle (\mathbf{x}^T H^2 \mathbf{x})^2 (\mathbf{x}^T H \mathbf{u})^2 \rangle &= \overset{1}{\sqcap} \overset{1}{\sqcap} \left| \frac{1}{2} \right| \left| \frac{1}{2} \right| = \overset{1}{\sqcap} \overset{1}{\sqcap} \overset{1}{\sqcap} \\
\langle (\mathbf{x}^T H \mathbf{u})^2 (\mathbf{u}^T H \mathbf{u})^2 \rangle &= \left| \frac{1}{2} \right| \left| \frac{1}{2} \right| \sqcup_1 \sqcup_1 = \sqcup_1 \sqcup_1 \sqcup_1 \\
\langle (\mathbf{x}^T H^2 \mathbf{u})(\mathbf{x}^T H \mathbf{u})^3 \rangle &= \left| \frac{3}{2} \right| \left| \frac{1}{2} \right| \left| \frac{1}{2} \right| \left| \frac{1}{2} \right| = 3 \sqcup_2 \sqcup_1 \\
\langle (\mathbf{x}^T H^2 \mathbf{x})(\mathbf{x}^T H \mathbf{u})^2 (\mathbf{u}^T H \mathbf{u}) \rangle &= \overset{1}{\sqcap} \left| \frac{1}{2} \right| \left| \frac{1}{2} \right| \sqcup_1 = \text{Tr}\{H\} \sqcup_1 \sqcup_1 + 2 \sqcup_2 \sqcup_1 \\
\langle (\mathbf{x}^T H^2 \mathbf{x})(\mathbf{x}^T H \mathbf{u})^4 \rangle &= \overset{1}{\sqcap} \left| \frac{1}{2} \right| \left| \frac{1}{2} \right| \left| \frac{1}{2} \right| \left| \frac{1}{2} \right| = 3 \overset{1}{\sqcap} \overset{1}{\sqcap} \overset{1}{\sqcap} \\
\langle (\mathbf{x}^T H \mathbf{u})^4 (\mathbf{u}^T H \mathbf{u}) \rangle &= \left| \frac{1}{2} \right| \left| \frac{1}{2} \right| \left| \frac{1}{2} \right| \left| \frac{1}{2} \right| \sqcup_1 = 3 \sqcup_1 \sqcup_1 \sqcup_1 \\
\langle (\mathbf{x}^T H \mathbf{u})^6 \rangle &= \left| \frac{1}{2} \right| \left| \frac{1}{2} \right| \left| \frac{1}{2} \right| \left| \frac{1}{2} \right| \left| \frac{1}{2} \right| \left| \frac{1}{2} \right| = 15 \sqcup_1 \sqcup_1 \sqcup_1.
\end{aligned} \tag{53}$$

In the first line, there is just one possible contraction. It connects the free ends in the bottom and the free ends on the top. The resulting closed loop has the total charge $3/2+3/2 = 3$. In the second line, there is only one possible contraction on the bottom. It connects the ends of the $3/2$ and $1/2$ lines. Their combined charge is now $3/2+1/2 = 2$. The other cases are simplified similarly. We are now left with computing:

$$\begin{aligned}
\overset{1}{\sqcap} \overset{1}{\sqcap} &= \text{Tr}\{H\}^2 + 2 \text{Tr}\{H^2\} \\
\overset{2}{\sqcap} \overset{1}{\sqcap} &= \text{Tr}\{H\} \text{Tr}\{H^2\} + 2 \text{Tr}\{H^3\} \\
\overset{1}{\sqcap} \overset{1}{\sqcap} \overset{1}{\sqcap} &= \text{Tr}\{H\}^3 + 6 \text{Tr}\{H\} \text{Tr}\{H^2\} + 8 \text{Tr}\{H^3\}.
\end{aligned} \tag{54}$$

In the first line, there is one contraction which connects the free ends 1-2 and 3-4. This gives two closed loops with charges $+1$, so the contribution of this term is $\text{Tr}\{H\}^2$. The contractions 1-3, 2-4 and 1-4, 2-3 both give one closed loop with the total charge $+2$, so they each contribute $\text{Tr}\{H^2\}$. The other diagrams are computed similarly.

Appendix C: Proof of Lemma 1

We here prove Lemma 5.1.

Proof. For the Δ 's numerator, we have

$$d^{-1} \cdot \text{Tr}\{H^3/d\} \leq \text{Tr}\{H/d\} \text{Tr}\{H^2/d\} \leq \text{Tr}\{H^3/d\}$$

and

$$d^{-2} \text{Tr}\{H^3/d\} \leq \text{Tr}\{H/d\}^3 \leq \text{Tr}\{H^3/d\}.$$

For the denominator, we have

$$d^{-1} \cdot \text{Tr}\{H^4/d\} \leq \text{Tr}\{H/d\} \text{Tr}\{H^3/d\} \leq \text{Tr}\{H^4/d\}$$

and

$$d^{-3} \text{Tr}\{H^4/d\} \leq \text{Tr}\{H/d\}^4 \leq \text{Tr}\{H^4/d\}.$$

And also $d^{-1/4} \leq \text{Tr}\{H^3/d\} / \text{Tr}\{H^4/d\}^{3/4} \leq 1$. This gives

$$\frac{3/4}{(10/4)^{3/4}} d^{-1/4} \leq \Delta \leq \frac{10/4}{(3/4)^{3/4}}.$$

□

References

- [1] Betancourt, M. (2017). “A conceptual introduction to Hamiltonian Monte Carlo.” *arXiv preprint arXiv:1701.02434*. 1
- [2] Blum, T., Boyle, P., Christ, N., Garron, N., Goode, E., Izubuchi, T., Lehner, C., Liu, Q., Mawhinney, R., Sachrajda, C., et al. (2011). “K to π π decay amplitudes from lattice QCD.” *Physical Review D*, 84(11): 114503. 14
- [3] Cuteri, F., Francis, A., Fritzsche, P., Pederiva, G., Rago, A., Shindler, A., Walker-Loud, A., and Zafeiropoulos, S. (2023). “Progress in generating gauge ensembles with Stabilized Wilson Fermions.” *arXiv preprint arXiv:2312.11298*. 14
- [4] Dalla Brida, M. and Lüscher, M. (2017). “SMD-based numerical stochastic perturbation theory.” *The European Physical Journal C*, 77: 1–16. 2
- [5] Doi, J. (2012). “Peta-scale lattice quantum chromodynamics on a Blue Gene/Q supercomputer.” In *SC'12: Proceedings of the International Conference on High Performance Computing, Networking, Storage and Analysis*, 1–10. IEEE. 14
- [6] Duane, S., Kennedy, A. D., Pendleton, B. J., and Roweth, D. (1987). “Hybrid monte carlo.” *Physics letters B*, 195(2): 216–222. 1, 2
- [7] Durmus, A. and Eberle, A. (2021). “Asymptotic bias of inexact Markov Chain Monte Carlo methods in high dimension.” *arXiv preprint arXiv:2108.00682*. 4
- [8] Grumitt, R. D., Dai, B., and Seljak, U. (2022). “Deterministic Langevin Monte Carlo with Normalizing Flows for Bayesian Inference.” *arXiv preprint arXiv:2205.14240*. 5, 12, 13

- [9] Hoffman, M. D., Gelman, A., et al. (2014). “The No-U-Turn sampler: adaptively setting path lengths in Hamiltonian Monte Carlo.” *J. Mach. Learn. Res.*, 15(1): 1593–1623. 3
- [10] Isserlis, L. (1918). “On a formula for the product-moment coefficient of any order of a normal frequency distribution in any number of variables.” *Biometrika*, 12(1/2): 134–139. 9
- [11] Janson, S. (1997). *Gaussian hilbert spaces*. 129. Cambridge university press. 9
- [12] Kantorovich, L. V. and Rubinshtein, S. (1958). “On a space of totally additive functions.” *Vestnik of the St. Petersburg University: Mathematics*, 13(7): 52–59. 4
- [13] Leimkuhler, B. and Matthews, C. (2015). “Molecular dynamics.” *Interdisciplinary applied mathematics*, 36. 2
- [14] Michalowicz, J., Nichols, J., Bucholtz, F., and Olson, C. (2009). “An Isserlis’ theorem for mixed Gaussian variables: Application to the auto-bispectral density.” *Journal of Statistical Physics*, 136: 89–102. 9
- [15] Minary, P., Martyna, G. J., and Tuckerman, M. E. (2003). “Algorithms and novel applications based on the isokinetic ensemble. I. Biophysical and path integral molecular dynamics.” *The Journal of chemical physics*, 118(6): 2510–2526. 8
- [16] Monmarché, P. (2022). “HMC and underdamped Langevin united in the unadjusted convex smooth case.” *arXiv preprint arXiv:2202.00977*. 5
- [17] Neal, R. M. et al. (2011). “MCMC using Hamiltonian dynamics.” *Handbook of markov chain monte carlo*, 2(11): 2. 1, 2
- [18] — (2011). “MCMC using Hamiltonian dynamics.” *Handbook of markov chain monte carlo*, 2(11): 2. 2, 3, 13
- [19] Olkin, I. and Pukelsheim, F. (1982). “The distance between two random vectors with given dispersion matrices.” *Linear Algebra and its Applications*, 48: 257–263. 4
- [20] Robbins, H. and Monro, S. (1951). “A stochastic approximation method.” *The annals of mathematical statistics*, 400–407. 3
- [21] Robnik, J., De Luca, G. B., Silverstein, E., and Seljak, U. (2022). “Microcanonical Hamiltonian Monte Carlo.” *arXiv preprint arXiv:2212.08549*. 2, 3, 7, 8, 10, 11, 12
- [22] Robnik, J. and Seljak, U. (2023). “Microcanonical Langevin Monte Carlo.” *arXiv preprint arXiv:2303.18221*. 2
- [23] Sountsov, P., Radul, A., and contributors (2020). “Inference Gym.” URL https://pypi.org/project/inference_gym 12
- [24] Ver Steeg, G. and Galstyan, A. (2021). “Hamiltonian Dynamics with Non-Newtonian Momentum for Rapid Sampling.” *Advances in Neural Information Processing Systems*, 34: 11012–11025. 8

- [25] Wick, G.-C. (1950). “The evaluation of the collision matrix.” *Physical review*, 80(2): 268. [9](#)